Investigating the effects of radiation, T cell depletion, and bone marrow transplantation on murine gut microbiota

Jakub Kreisinger[1], James Dooley[2], Kailash Singh[2,3],
Dagmar Čížková[4], Lucie Schmiedová[4], Barbora Bendová[1],
Adrian Liston[2] and Alena Moudra[2,5]*

[1]Department of Zoology, Faculty of Science, Charles University, Prague, Czechia, [2]Immunology
Programme, The Babraham Institute, Cambridge, United Kingdom, [3]Department of Medical Cell
Biology, Uppsala University, Uppsala, Sweden, [4]Institute of Vertebrate Biology, Czech Academy of
Sciences, Brno, Czechia, [5]The National Institute of Mental Health, Klecany, Czechia

Microbiome research has gained much attention in recent years as the importance of gut microbiota in regulating host health becomes increasingly evident. However, the impact of radiation on the microbiota in the murine bone marrow transplantation model is still poorly understood. In this paper, we present key findings from our study on how radiation, followed by bone marrow transplantation with or without T cell depletion, impacts the microbiota in the ileum and caecum. Our findings show that radiation has different effects on the microbiota of the two intestinal regions, with the caecum showing increased interindividual variation, suggesting an impaired ability of the host to regulate microbial symbionts, consistent with the Anna Karenina principle. Additionally, we observed changes in the ileum composition, including an increase in bacterial taxa that are important modulators of host health, such as *Akkermansia* and *Faecalibaculum*. In contrast, radiation in the caecum was associated with an increased abundance of several common commensal taxa in the gut, including *Lachnospiraceae* and *Bacteroides*. Finally, we found that high doses of radiation had more substantial effects on the caecal microbiota of the T-cell-depleted group than that of the non-T-cell-depleted group. Overall, our results contribute to a better understanding of the complex relationship between radiation and the gut microbiota in the context of bone marrow transplantation and highlight the importance of considering different intestinal regions when studying microbiome responses to environmental stressors.

KEYWORDS

HSC, T cell depleted, BM transplantation, T cell replete, microbiome and dysbiosis

Introduction

The gut microbiota has a massive impact on host health and affects outcomes of various medical treatments through the production of a wide range of bioactive molecules and/or interactions with host tissues and the immune system. Despite extensive research on the changes in the gut microbiota following exposure to ionizing radiation, the microbiota's specific role in murine bone marrow transplantation (BMT) remains poorly understood. Total-body irradiation, which is a common component of the conditioning regimen for BMT,

can induce dose-dependent damage to the gut, leading to dysbiosis of the microbiota and a decrease in microbial diversity (Staffas et al., 2017).

When exposed to ionizing radiation, certain tissues, including the gut epithelia, which have a high rate of cell proliferation, are particularly vulnerable to damage (Cui et al., 2017). The damaged intestinal epithelial cells resulting from radiation can lead to compromised barrier function and contribute to bacterial dysbiosis and depletion of butyrate-producing bacteria (Parada Venegas et al., 2019). Butyrate, a short-chain fatty acid produced by gut bacteria, serves as the primary energy source for repair-promoting intestinal epithelial cells (IECs). Its depletion can lead to several consequences, including compromised epithelial barrier function, increased pro-inflammatory cytokines, dysregulation of the epithelial immune response, and altered microbial balance (Liu et al., 2021). On the other hand, the presence of specific microbiota species capable of mitigating radiation-induced tissue damage by producing anti-inflammatory molecules predicts better survival and recovery after irradiation (Guo et al., 2020).

The effect of radiation has been studied primarily on bacterial communities inhabiting the lower intestine (i.e., caecum and colon). However, little is known about the effects of radiation on the gut microbiota outside the lower gut, which has a different taxonomic composition (Moudra et al., 2021) and mediates specific functions for the host (Zoetendal et al., 2012; Kastl et al., 2020).

In allogeneic hematopoietic stem cell transplantations (HCT), the transplanted immune cells may identify the recipient's healthy tissues as foreign, resulting in the onset of graft-versus-host disease (GVHD). This complication leads to mortality in 15.9% of individuals who undergo allogeneic HCT (Styczyński et al., 2020). Intestinal microbiota plays a crucial role in developing GVHD and HCT outcomes (Fredricks, 2019). Studies using allogeneic BMT mouse models have characterized the exaggerated inflammatory mechanisms that lead to acute GVHD in target organs (Jenq et al., 2012; Staffas et al., 2017). These studies have demonstrated that alterations in the composition and diversity of the gut microbiota can disrupt immune homeostasis and contribute to the pathogenesis of GVHD. One common way to prevent GVHD is T-cell depletion of the donor bone marrow cells (Daniele et al., 2012). Most early trials documented that T-cell depletion could substantially limit acute and chronic GVHD (Ho and Soiffer, 2001). While there is no direct evidence linking T-cell depletion to changes in the microbiota, it is known that GVHD, which can be prevented by T-cell depletion, can cause severe inflammation and damage to the gut (Katiraei et al., 2022). Overall, the impact of T-cell depletion during bone marrow transplantation on the microbiota is an area that requires further research.

The gut microbiota has been shown to modulate the human immune system, and its impact on HCT outcomes and transplant rejection risk has been increasingly recognized (Zama et al., 2020; Sen and Thummer, 2022). Research in human cohorts has revealed that the composition of the gut microbiota prior to transplantation can influence the likelihood of GVHD development and the overall success of the transplant. Specifically, dysbiosis, characterized by an imbalance in the relative abundance of microbial species, has been associated with increased GVHD incidence and reduced survival rates following transplantation. Recent studies have also highlighted the emerging role of gut microbiota and its metabolites in profoundly impacting allogeneic hematopoietic stem cell transplantation (Kouidhi

et al., 2021). These studies have shown that the gut microbiota can influence the efficacy of the transplantation process, including engraftment and immune reconstitution (Miltiadous et al., 2022). Moreover, specific microbial metabolites, such as short-chain fatty acids, have been implicated in regulating immune responses and promoting the tolerance of donor cells.

To address the above knowledge gaps, we designed an experiment to evaluate the effects of radiation and T-cell depletion separately. By exposing congenic mice to different doses of radiation, we also investigated the mutual interactions between radiation and T-cell depletion on the resulting composition of the gut microbiota. Last but not least, in addition to the microbiota of the lower intestine represented by caecum samples, we also analyzed the microbiota communities in the ileum. In this way, we were able to gain a unique insight into the effects of BMT (and ionizing radiation in general) on the microbiota of the small intestine. We present the major conclusions of our investigation into the effects of radiation and subsequent bone marrow transplantation with or without T cell depletion on the microbiota of the ileum and caecum using the congenic bone marrow C57Bl6/J mouse model.

Main findings

- Combined effect of radiation and antibiotics treatment has different effects on the microbiota of the ileum and the caecum.
- In the caecum, interindividual variation increases due to the combined effect of antibiotics treatment, radiation and BMT, indicating the impaired ability of the host to regulate microbial symbionts [also known as the Anna Karenina principle (Zaneveld et al., 2017)].
- Changes in ileum composition include bacterial taxa that are important modulators of host health: *Akkermansia* [anti-inflammatory effect (Cani et al., 2022)] *Faecalibaculum* [antitumor effect (Zagato et al., 2020)].
- In the caecum, radiation is associated with an increased abundance of common commensal taxa in the gut, e.g., *Lachnospiraceae* and *Bacteroides*.
- High doses of radiation have more substantial effects on the caecal microbiota of the T cell-depleted group than that of the non-T cell-depleted group.

Methods

Experimental animals

C57BL/6.SJL-*Ptprc^a*/BoyJ (CD45.1) mice were bred and maintained in the Babraham Institute Biological Support Unit (BSU).

No primary pathogens or additional agents listed in the FELASA recommendations (Mähler Convenor et al., 2014) were detected during health-monitoring surveys of the stock holding rooms. The ambient temperature was ~19–21°C, and the relative humidity was 52%. Lighting was provided on a 12-h light: 12-h dark cycle, including 15 min 'dawn' and 'dusk' periods of subdued lighting. After weaning, mice were transferred to individually ventilated cages with 1–5 mice per cage. Mice were fed CRM (P) VP diet (Special Diet Services) *ad*

libitum and received seeds (e.g., sunflower, millet) at the time of cage cleaning as part of their environmental enrichment. The Babraham Institute Animal Welfare and Ethical Review Body approved all the mouse experimentation. Animal husbandry and experimentation complied with existing European Union and United Kingdom Home Office legislation and local standards (PPL: PP3981824).

Sample sizes for mouse experiments were chosen in conjunction with the ethics committees to allow for robust sensitivity without excessive use. Males and females were used for experiments. Age- and sex-matched pairs of animals were used in the experimental groups. Where possible, littermates were equally divided into the experimental groups.

Bone marrow chimeras

For the bone marrow (BM) reconstitution experiment, CD45.1 mice were exposed to varying doses of radiation (refer to Supplementary Table S1 for detailed doses) and subsequently intravenously reconstituted with $2–5 \times 10^6$ freshly-collected total BM cells from C57Bl/6 donor mice. The radiation source employed was Cesium 137, delivered by the Schering machine, Model IBL 437C. Mice were positioned in irradiation pots within a canister that rotates past the source during irradiation. The duration required to deliver one Gray (Gy) of radiation is variable due to the degradation of the source, presently set at 15 s per Gy.

The BM cells were obtained by crushing the tibia and fibula using a mortar and pestle, followed by filtration through a 50-um filter and red blood cell (RBC) lysis. The total cell count was determined using a hemocytometer. The resulting BM mixture was subjected to T cell depletion using CD4 and CD8 T cell MicroBeads (Miltenyi, cat. No. 130–117-043 and 130–117-044) or injected without T cell depletion.

To prevent infections, the experimental animals undergoing bone marrow transplantation (BMT) were treated with the fluoroquinolone-type antibiotic enrofloxacin (Baytril, Bayer) (50 mg/mL) in their water bottle for the initial 3 weeks after irradiation, following the standard protocol. The mice were allowed 10 weeks after BMT for BM reconstitution, providing a 7-week window for microbiome reconstitution. The well-being of the experimental animals was monitored daily, and mice that exhibited a weight loss of 20% or showed moderate signs of stress (such as intermittent hunching, piloerection, reduced activity, or poor grooming) were euthanized on ethical grounds. Animals affected by the treatment procedure were excluded from the final dataset.

Upon completion of the experiment, the animals were euthanized, and samples from the duodenum, jejunum, ileum, caecum, and colon were collected for high-throughput 16S rRNA sequencing of the intestinal microbiota.

Treatment groups

The following numbers of animals were used for the experiments - high radiation dose 10–13 Gy (depleted males $n = 11$, depleted females $n = 14$, non-depleted males $n = 10$, non-depleted females $n = 11$), low radiation dose 4–5.5 Gy (depleted males $n = 12$, non-depleted males $n = 12$), control untreated animals (males $n = 7$, females $n = 5$), see Supplementary Table S1 for details.

Sample preparation

Experimental animals were euthanized, and approximately 1.5 cm of the caecal tip and ileum were excised from each individual and placed on separate sterile Petri dishes. The contents of the intestinal samples were carefully squeezed out and the intestinal tissue was then placed in cryotubes filled with 96% ethanol for later analysis (VWR, 20821.330P). Clean and fire-sterilized scissors and forceps were used for each intestinal section to minimize bacterial DNA contamination. A negative control cryotube was prepared for each round of dissections to sample the possible air-borne contamination. The ileum, caecum, and colon were sampled separately, with the contents and walls placed in separate cryotubes and frozen at −80°C. An additional fecal sample was taken from the last portion of the colon.

Sample processing

Metagenomic DNA was extracted using the PowerSoil kits (QIAGEN). Gut microbiome sequencing libraries were prepared using the two-step PCR protocol at the Studenec Research Facility of the Institute of Vertebrate Biology, CAS, as described in detail in Čížková et al. (2021). Briefly, standard metabarcoding primers for the V3-V4 hypervariable region of bacterial 16S rRNA (Klindworth et al., 2013) were used in the first PCR step to amplify the specific rRNA loci. Dual indexes were introduced in the second PCR, during which Illumina-compatible Nextera-like sequencing adaptors were reconstituted. Each metabarcoding PCR was performed in a technical duplicate to account for the stochasticity of PCR and sequencing. PCR products were pooled according to their concentration, and pools were sequenced using Illumina Miseq (v3 kit, 300 bp paired-end reads) at CEITEC, Brno, Czech Republic.

Bioinformatics

Skewer (Jiang et al., 2014) was used to demultiplex samples and detect and trim gene-specific primers. In the next step, low-quality reads (expected error rate per paired-end read >2) were eliminated, quality-filtered reads were denoised, and abundance matrices were generated using the read counts for each 16S rRNA amplicon sequencing variant (hereafter ASVs) in each sample. All these steps were performed using the R package dada2 (Callahan et al., 2016). Subsequently, uchime (Edgar et al., 2011) was used in conjunction with the gold.fna reference database[1] to detect and eliminate chimeric ASVs. The taxonomy for the non-chimeric ASVs was assigned with 80% posterior confidence by the RDP classifier (Wang et al., 2007) using the Silva database v.138 (Quast et al., 2013) as a reference. Procrustean analysis revealed high consistency between technical duplicates ($r = 0.97$, $p = 0.0001$). Consequently, we merged the microbiota profiles of the technical duplicates, eliminating all ASVs that were not detected in both duplicates. Finally, we excluded all samples with a number of high-quality reads <1,000.

---

1   Available at: https://drive5.com/uchime/gold.fa

The final dataset included data from 82 mice whose gut microbiota was sequenced. We were unable to sequence two ileum samples due to insufficient concentration of template DNA, so the final data set included a total of 182 samples (82 from the caecum and 80 from the ileum). The total number of sequences for the entire data set was 1,599,231, with an average sequencing coverage per sample of 9,872 (range = 1,532–19,507). A total of 1,016 bacterial ASVs were detected. Sample metadata for this study is shown in Supplementary Table S1.

The final dataset was used for metagenome predictions using the picrust2 pipeline (Douglas et al., 2020) with default parameters, where predicted metagenomes were categorized into functional pathways (Ye and Doak, 2009). Using the BugBase pipeline, we also estimated the frequency of selected phenotypic traits for each sample, including, for example, stress and oxygen tolerance, pathogenicity potential, biofilm formation ability, or Gram positivity/negativity (Ward et al., 2017).

Statistics

The microbiota of the caecum was clearly different from the microbial profiles of the ileum (Supplementary Figure S1). Therefore, we analyzed these two sample types separately. For the entire data set, we first tested whether the microbiota differed between experimental groups (non-irradiated controls vs. irradiated depleted and irradiated non-T cell-depleted mice) using mixed effects models. The effect of sex and experimental replicate were included as covariates, and cage identities as random effects. In the subsequent analysis step, we removed the control individuals (who were not irradiated and did not receive antibiotics treatment, $n = 12$) from the data to examine the effect of radiation dose. Because of the dichotomous distribution of radiation doses, in which mice were exposed to relatively low doses between 4.5 and 5.5 Gy ($n = 24$) or high radiation doses between 10 and 13 Gy ($n = 46$), we considered these two categories as a factorial predictor. Apart from the effect of radiation dose and the set mentioned above of covariates, we also tested whether the effect of radiation dose differed between the depleted and non-T-cell-depleted groups by including an interaction term in these statistical models.

Statistical analyses considered three levels of microbiota variation. First, we focused on alpha diversity variation, assessed based on the Shannon diversity index and ASV richness (i.e., the total number of ASVs) calculated for each sample. These alpha diversity indices were considered response variables in mixed models with Gaussian error distribution fitted with the R package lme4. To achieve a normal distribution of the residuals, $\log_{10}$-transformed values of ASV richness were used.

Next, variation in microbiota composition was analyzed using mixed models from the R package MDMR (McArtor et al., 2017), with compositional dissimilarity between samples as the response. Two dissimilarity indices were considered: the Jacccard index, which considers only variation in the presence/absence of ASV, and the Bray-Curtis index, which also considers variation in relative ASV abundances. We focused on systematic shifts in the community and analyzed differences in interindividual dispersion between experimental groups. For these analyses, we calculated Euclidean distances to centroids of each of the three experimental groups using the betadisper function from the R package vegan. Consequently, individuals with highly divergent microbiota content compared with other individuals within the same experimental group received high

scores. Distances to centroids were $\log_{10}$-transformed and then used as response variables in mixed models fitted with the R package lme4. Finally, we examined variation in the relative abundance of individual ASVs using mixed models with negative binomial distribution fitted with the R package glmmTMB, using the number of reads for each ASV in each sample as the response variable. To avoid false positives due to multiple testing, we calculated false discovery rates (FDR) (Benjamini and Hochberg, 1995) based on the resulting probability values and considered only those results as significant where the FDR was less than 0.05.

To account for differences in sequencing depth between samples, we included log-transformed read counts for each sample at the model offset in the ASV-level analyses. In the case of the alpha-diversity and dissimilarity-based analyses, diversity indices were calculated based on rarefaction datasets, with the rarefaction threshold corresponding to the minimum sequencing depth achieved.

Statistical analyses of metagenome predictions followed a similar logic, with two exceptions. First, alpha diversity analyses were not performed for the predicted metagenomes. Second, we did not consider absence/presence-based Jaccard dissimilarity, as it is less informative given the functional redundancy of microbial communities.

For the data analysis, we employed version R-4.3.2 of the R software.

Results

Variation in alpha diversity

For the entire data set of microbial profiles of the caecum and ileum, we did not detect any effects of radiation or radiation combined with depletion on microbial alpha diversity. The same was true for all other predictors tested, including the experimental replicate (Supplementary Table S2). After excluding control mice from the data set, significant interactions between depletion treatment and radiation dose indicated a differential suggested divergent effect of radiation intensity on alpha diversity of caecum microbiota in depleted versus non-T cell-depleted mice. However, there were no effects of radiation dose or other covariates on the ileum microbiota (Supplementary Table S3). Separate models for non-T cell-depleted mice showed an increase in alpha diversity of the caecal microbiota in non-T-cell-depleted mice exposed to higher radiation doses (ASV richness: Estimate = 0.0550 ± 0.0246 [± SE], ΔD.f. = 1, $\chi^2 = 5.2462$, $p = 0.0220$, Shannon: Estimate = 0.2237 ± 0.0837 [± SE], ΔD.f. = 1, $\chi^2 = 7.89$, $p = 0.0050$), whereas there was no such difference in depleted individuals (ASV richness: Estimate = −0.0240 ± 0.0387 [± S.E.], ΔD.f. = 1, $\chi^2 = 0.5859$, $p = 0.4440$, Shannon: Estimate = −0.1391 ± 0.1223 [± SE], ΔD.f. = 1, $\chi^2 = 1.9432$, $p = 0.1633$).

Variation in composition
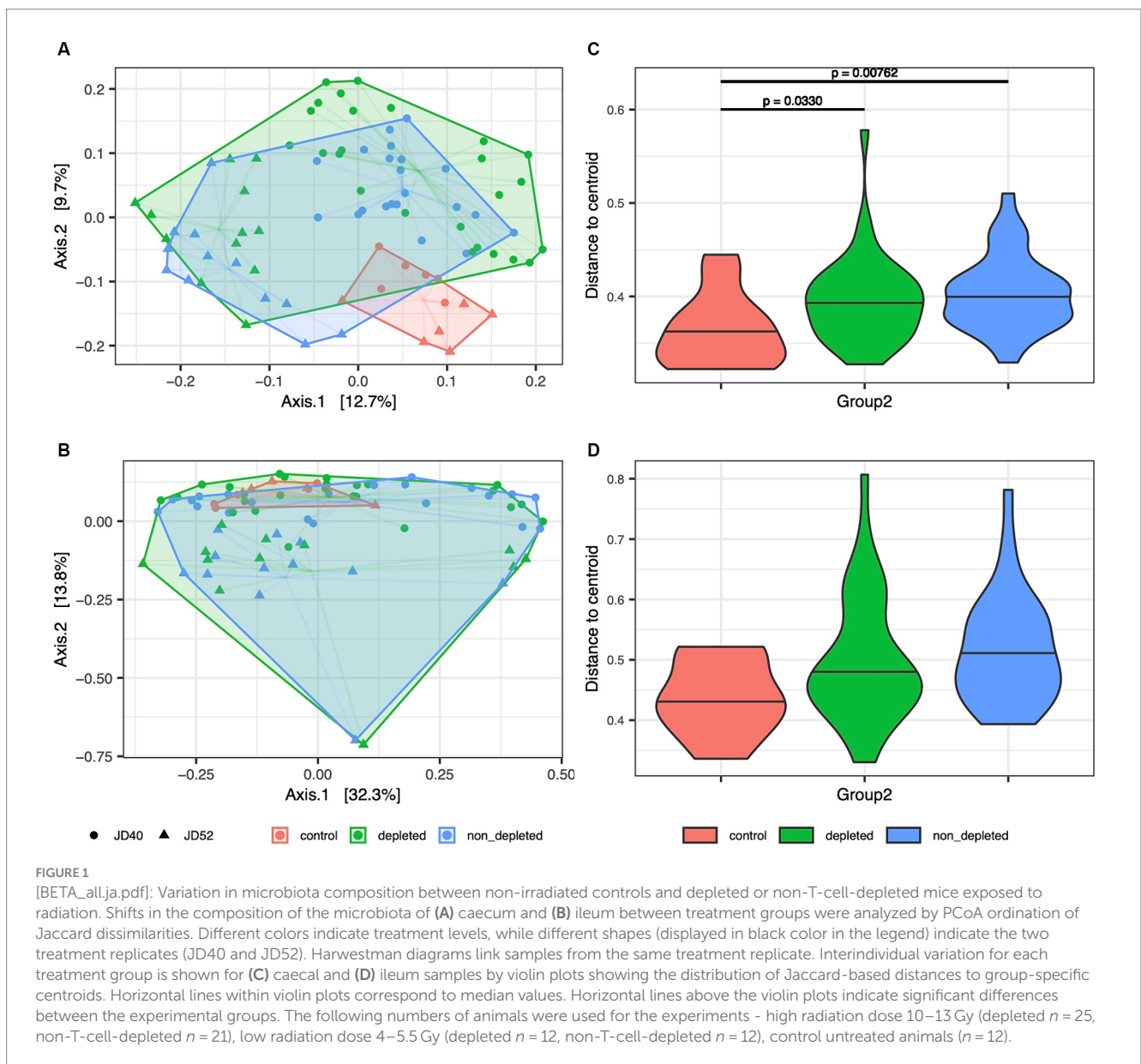
After statistically controlling for variation between experimental replicates and other confounding factors, both irradiated groups' caecum and ileum microbiota showed significant compositional changes compared with non-irradiated controls without antibiotics (Supplementary Table S4; Figure 1). This was also confirmed by additional MDMR analyses aimed at pairwise comparisons of all

treatment groups, which consistently revealed significant differences between controls and depleted mice or controls and non-T-cell-depleted mice ($p < 0.01$ in all cases). In contrast, differences between depleted and non-T-cell-depleted mice were insignificant ($p > 0.1$ in all cases). In addition to the effects of radiation, antibiotics and BMT on microbiota composition, both MMDR analyses and PCoA-based sample ordination (Figure 1; Supplementary Table S4) showed considerable changes between experimental replicates. While the microbiota of the control group was comparable in both replicates, the microbiota of both irradiated mice showed a pronounced divergence greater than the variation between irradiated and non-irradiated mice within the experimental replicates (Supplementary Table S4).

Apart from the systematic compositional shifts due to radiation and subsequent course of enrofloxacin antibiotic treatment revealed by MDMR analyses, PCoA (Figure 1) also suggested that the irradiated mice exhibited increased interindividual dispersion, as indicated by a larger ordination space occupied. This pattern may result from perturbed mechanisms regulating the symbiotic microbiota. The

administration of a broad-spectrum antibiotic enrofloxacin causes a state of dysbiosis in which there is an elevated proportion of *Clostridium coccoides*, *C. coccoides-Eubacterium rectale*, *Bacteroidetes*, and *Bifidobacterium* spp., while the presence of segmented filamentous bacteria is reduced (Aguilera et al., 2015).

To statistically test this type of variation, linear mixed models were fitted, where Euclidean distances to PCoA centroids for sample groups determined by the combination of treatment level and experimental repetition were included as a response. For the Jaccard index and caecum microbiota, this approach revealed increased interindividual dispersion of both irradiated groups compared with the control (Figure 1; Supplementary Table S5). In contrast, for the Bray-Curtis dissimilarities, the difference between the controls and T-cell-depleted mice was only marginally significant ($p = 0.0799$). In the case of ileum microbiota, the differences in interindividual dispersion between experimental groups were only marginally significant when Jaccard dissimilarities were considered and not significant for Bray-Curtis dissimilarities (Supplementary Table S5).

FIGURE 1
[BETA_all.ja.pdf]: Variation in microbiota composition between non-irradiated controls and depleted or non-T-cell-depleted mice exposed to radiation. Shifts in the composition of the microbiota of **(A)** caecum and **(B)** ileum between treatment groups were analyzed by PCoA ordination of Jaccard dissimilarities. Different colors indicate treatment levels, while different shapes (displayed in black color in the legend) indicate the two treatment replicates (JD40 and JD52). Harwestman diagrams link samples from the same treatment replicate. Interindividual variation for each treatment group is shown for **(C)** caecal and **(D)** ileum samples by violin plots showing the distribution of Jaccard-based distances to group-specific centroids. Horizontal lines within violin plots correspond to median values. Horizontal lines above the violin plots indicate significant differences between the experimental groups. The following numbers of animals were used for the experiments - high radiation dose 10−13 Gy (depleted $n = 25$, non-T-cell-depleted $n = 21$), low radiation dose 4−5.5 Gy (depleted $n = 12$, non-T-cell-depleted $n = 12$), control untreated animals ($n = 12$).

Additional analyses were performed for a data subgroup without non-irradiated controls to determine whether the microbiota changed with radiation dose and whether this change was modulated by depletion treatment. There was only a mild significant effect of radiation dose on the ileum microbiota when Jaccard dissimilarities were used, and there was an effect on the ileum microbiota based on Bray-Curtis dissimilarities. However, a highly significant interaction between depletion treatment and radiation dose in the caecum samples suggested a differential effect of radiation intensity in T-cell-depleted versus non-T-cell-depleted mice (Supplementary Table S6). In a separate analysis for the subset of caecum samples from the T-cell-depleted mice, the effect of radiation dose was highly significant (MDMR: D.f. = 1, MDMR statistic = 20.7289, $p < 0.0001$ for Bray-Curtis and D.f. = 1, MDMR statistic = 5.7491, $p < 0.0001$ for Jaccard dissimilarities) and that the same was true for non-T-cell-depleted groups (MDMR: D.f. = 1, MDMR statistic = 4.8182, $p < 0.0001$ for Bray-Curtis and D.f. = 1, MDMR statistic = 1.8816, $p = 0.0172$ for Jaccard dissimilarities), although the effect size was much smaller. This was consistent with the PCoA sample ordination (Figure 2), in which the depleted mice exposed to high and low doses of radiation formed almost no overlapping clusters. In contrast, considerable overlap was observed in the non-T-cell-depleted group exposed to different doses of radiation.

Variation in ASVs relative abundances

Differential abundance analyses comparing the caecal microbiota of the non-irradiated controls with that of the two irradiated groups identified five ASVs from the genus *Bacteroides* and the family

FIGURE 2
[Jac_dose.pdf]: PCoA ordination of Jaccard dissimilarities depicts variation in caecum microbiota composition between depleted and non-T-cell-depleted mice exposed to either high or low doses of radiation. The following numbers of animals were used for the experiments - high radiation dose 10−13 Gy (depleted n = 25, non-T-cell-depleted n = 21), low radiation dose 4−5.5 Gy (depleted n = 12, non-T-cell-depleted n = 12).

Lachnospiraceae whose relative abundance was increased in the irradiated mice. Complementary analyses for the ileum microbiota revealed a decreased abundance of *Faecalibaculum* and *Muribaculum* and an increased abundance of *Akkermansia* in the mice exposed to radiation and subsequent antibiotics treatment (Figure 3).

Differential abundance analyses for the caecal microbiota, testing the effect of radiation dose, revealed different ASVs variation patterns for the T-cell-depleted and non-T-cell-depleted mice. For the subgroup of T-cell-depleted mice, high radiation doses resulted in an increased abundance of ASVs from *Lachnospiraceae* and *Oscillospiraceae*, whereas ASVs from the genus *Oscillospira* and the family *Muribaculaceae* showed the opposite direction of change. On the other hand, non-T-cell-depleted mice exposed to high radiation and subsequent antibiotics treatment showed an increased abundance of ASVs from the genus *Lactobacillus* and decreased abundance of ASVs from the genus *Alistipes* and *Lachnospiraceae* (Figure 4).

Predicted microbiota functions

According to MDMR analyses, the content of caecal metagenomes differed between non-irradiated controls and depleted (Tukey posthoc tests: $p < 0.0001$) or non-T-cell-depleted (Tukey posthoc tests: $p = 0.0004$) mice, both of which were exposed to radiation. However, experimental groups had no significant differences in predicted metagenomes of the ileum microbiota (Supplementary Table S4; Supplementary Figure S4). This was consistent with differential abundance analyses identifying 14 metabolic pathways, whose predicted abundances differed between controls and irradiated groups (Supplementary Figure S6). Interindividual variation did not vary significantly between experimental groups (Supplementary Table S5), although PCoA indicated increased interindividual variation in mice exposed to radiation (Supplementary Figure S4). MDMR for a data set without non-irradiated controls showed that radiation dose significantly altered the caecum microbiome but not the ileum (Supplementary Figure S5; Supplementary Table S5). In addition, consistent with the same analyses for microbiota composition, the interaction between radiation dose and depletion treatment was significant for caecum microbiota. Differential abundance analyses identified five predicted pathways for depleted and 34 pathways for non-T-cell-depleted groups, whose expression varied with radiation dose. However, estimates characterizing abundance changes between mice exposed to high vs. low radiation intensity calculated separately for depleted and non-T-cell-depleted groups were tightly correlated ($r = 0.6693$, $p < 0.00001$).

BugBase predictions revealed no differences between experimental groups in the proportion of aerobic, facultative aerobic, Gram-negative, stress-tolerant, or potentially pathogenic bacteria and bacteria that can form biofilms (Supplementary Figure S8; LMM: $p > 0.05$ in all case).

Discussion

Our study aimed to shed light on the complex relationship between radiation, BM transplantation, and gut microbiota. We specifically focused on the ileum and caecum as these regions have distinct functions and harbor different microbial communities (Zoetendal et al., 2012; Kastl et al., 2020). Our findings suggest that radiation and subsequent antibiotic treatment have different effects on
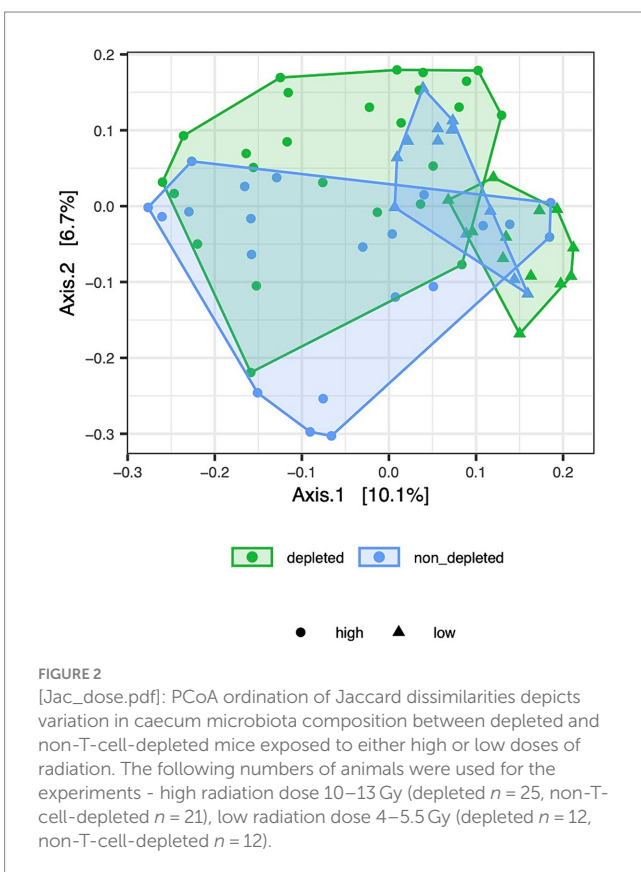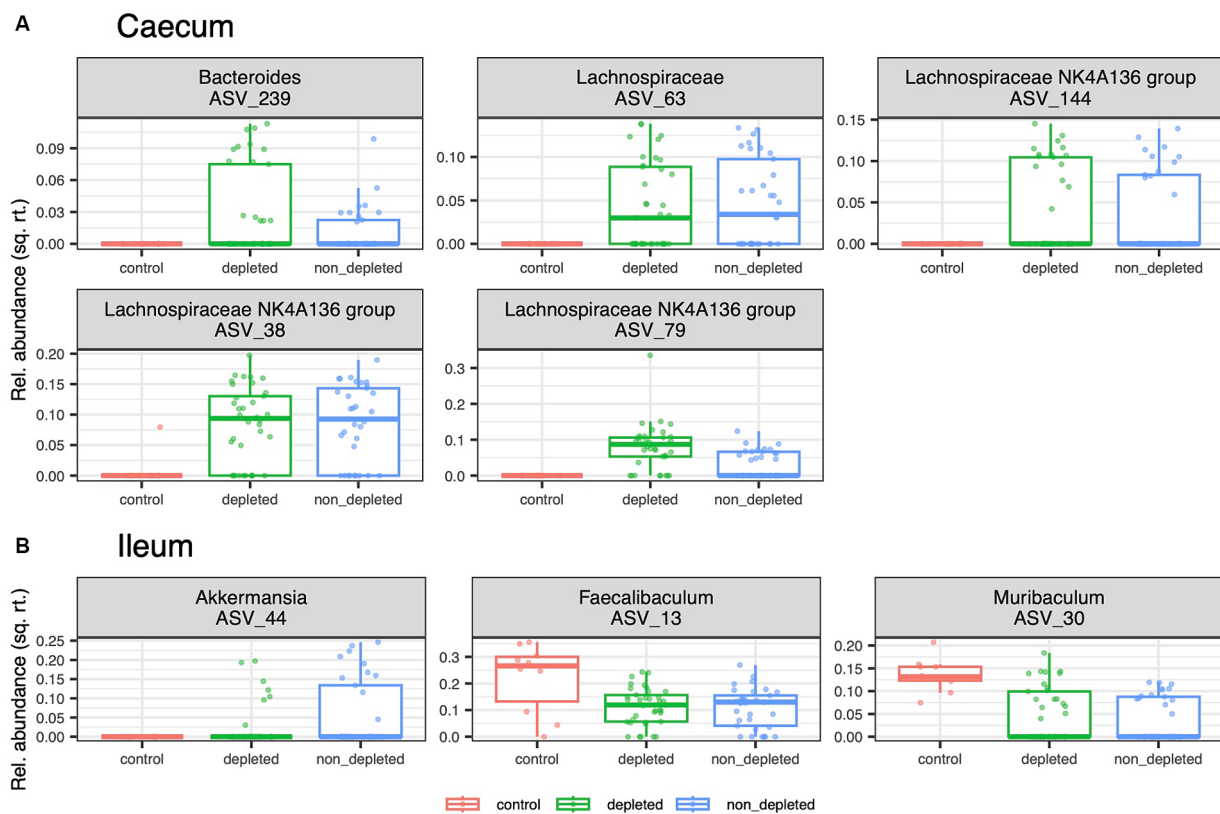
FIGURE 3
[DFA_all.pdf]: Effect of radiation on ASVs relative abundances. Box plots showing a variation of ASVs whose relative abundance in **(A)** caecum and **(B)** ileum microbiota differs among three treatment groups represented by non-irradiated controls, irradiated depleted mice, and irradiated non-T-cell-depleted mice. The following numbers of animals were used for the experiments - high radiation dose 10−13 Gy (depleted $n = 25$, non-T-cell-depleted $n = 21$), low radiation dose 4−5.5 Gy (depleted $n = 12$, non-T-cell-depleted $n = 12$), control untreated animals ($n = 12$).

the microbiota of these two intestinal regions. In particular, we found that 10 weeks after BMT the irradiated caecum exhibited increased interindividual variation and impaired ability of the host to regulate microbial symbionts, consistent with the Anna Karenina principle. Similarly, examination of the caecal microbiome composition 24 weeks after the BMT showed high degree of inter-individual variation but no consistent longitudinal changes induced by the BMT (Katiraei et al., 2022). These observations suggest that radiation and subsequent antibiotic treatment may significantly impact the stability and functionality of the caecal microbiota.

Our study revealed noteworthy changes in the microbiome composition of the ileum, the last section of the small intestine, following radiation exposure and subsequent antibiotics treatment. Specifically, we found an increase in the abundance of certain bacterial taxa, such as *Akkermansia*, which are crucial in maintaining host health. In contrast, we observed a decrease in the *Faecalibaculum* and *Muribaculum*.

Of particular interest, *Akkermansia* has been shown to have numerous benefits, including enhancing glucose metabolism, promoting intestinal barrier function, and exerting anti-inflammatory effects (Cani et al., 2022). Meanwhile, *Faecalibaculum* has been associated with antitumor properties and the production of short-chain fatty acids that facilitate the production of IgA by plasma cells (Zagato et al., 2020). Interestingly, the levels of *Akkermansia* and *Faecalibaculum* in the gut microbiota have been found to positively correlate with the hypoglycemic effects of *Astragalus membranaceus* polysaccharides and the alleviation of food allergy symptoms in mice

(Lu et al., 2022; Song et al., 2022). Our findings support the crucial role of *Akkermansia* and *Faecalibaculum* in gut microbiota-mediated host health responses and suggest that radiation exposure may impact these important microbial populations.

Comparatively, in humans, after allogeneic BMT, there is a decline in bacterial alpha diversity within the first 3 weeks in the gut, oral, and nasal microbiota (Taur et al., 2012; Kaysen et al., 2017; Ingham et al., 2019, 2021; Peled et al., 2020). Both mouse models and patients with acute GVHD exhibit the most significant loss of diversity (Jenq et al., 2012; Taur et al., 2012; Holler et al., 2014; Mancini et al., 2017; Peled et al., 2020). It is noteworthy that both adult and pediatric allo-BMT patients experience reduced diversity and an altered gut bacterial composition even before conditioning and transplantation, compared with healthy individuals (Peled et al., 2020; Ingham et al., 2021). This reduction in diversity may be due to antibiotic treatment, which reduces specific groups of commensal mucosal colonizers. Obligate anaerobes, such as *Clostridiales*, *Negativicutes*, *Bacteroidetes*, and *Fusobacteria*, are reported to be especially vulnerable to the adverse effects of Piperacillin-tazobactam and meropenem. In contrast, fluoroquinolones, intravenous vancomycin, and trimethoprim-sulfamethoxazole appear to have a lesser impact on these bacterial groups (Morjaria et al., 2019; Weber et al., 2019).

However, we also found that radiation and antibiotics treatment in the caecum was associated with an increased abundance of several common commensal taxa in the gut 7 weeks after antibiotics treatment cessation, including *Lachnospiraceae* and *Bacteroides*. This
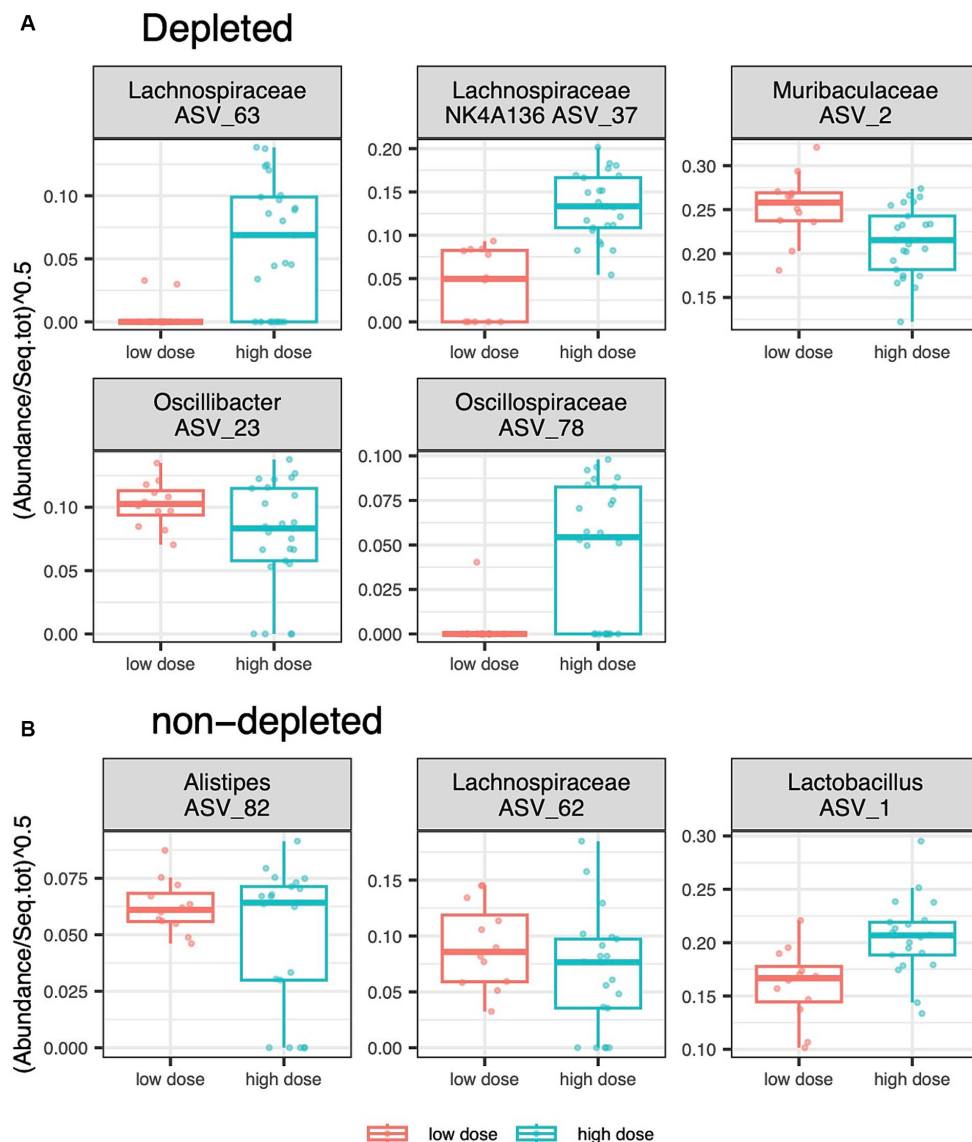
FIGURE 4

[DFA_depl_nondepl.pdf]: Effect of radiation dose and depletion treatment on ASVs relative abundances. Boxplots showing the variation of ASVs whose relative abundance in the caecum of **(A)** the depleted group and **(B)** the non-T-cell-depleted group differed between individuals exposed to a low and a high radiation dose.The following numbers of animals were used for the experiments - high radiation dose 10–13 Gy (depleted $n = 25$, non-T-cell-depleted $n = 21$), low radiation dose 4–5.5 Gy (depleted $n = 12$, non-T-cell-depleted $n = 12$).

observation suggests that radiation and subsequent antibiotics treatment may impact the composition of the caecal microbiota differently, depending on the microbial taxa involved. Similarly, increased abundance of both *Lachnospiraceae* and *Bacteroides* has been shown to ameliorate the acute GVHD in allo-BMT patients (Eriguchi et al., 2012; Biagi et al., 2015, 2019; Doki et al., 2017; Payen et al., 2020). Conversely, the mouse model of aGVHD has shown a reduction of Bacteroidetes 2 weeks after BMT (Jenq et al., 2012).

Finally, we found that high doses of radiation had more substantial effects on the caecal microbiota of the depleted group than that of the non-T-cell-depleted group. The increased abundance of acute GVHD ameliorating *Lachnospiraceae* in the T-cell depleted group of BMT highlights the importance of considering the role of immune cells in modulating the gut microbiota in response to environmental stressors.

In conclusion, our study provides valuable insights into the effects of radiation and bone marrow transplantation on the gut microbiota in the murine BM transplantation model. Our findings suggest that radiation and the subsequent antibiotics treatment have different effects on the ileum and caecum microbiota and that immune cells' role in modulating the gut microbiota should be considered when studying responses to environmental stressors. Further research is needed to fully understand the complex interactions between radiation, gut microbiota, and host health.

Conclusion

This study investigated the relationship between radiation, bone marrow transplantation (BMT), and gut microbiota in the ileum and

caecum. The irradiated caecum showed increased interindividual variation and impaired microbial regulation. Radiation and antibiotics treatment had varying effects on the ileum, with an increase in beneficial bacteria like *Akkermansia* and a decrease in *Faecalibaculum*. *Akkermansia* and *Faecalibaculum* play important roles in host health. Human BMT patients also experience bacterial diversity and composition changes, particularly in graft-*vs*-host disease (GVHD) cases. In the caecum, radiation and antibiotics treatment increased the abundance of specific commensal taxa. The impact of radiation on the caecal microbiota was more pronounced in the T-cell-depleted group showing that the immune cells influence the gut microbiota's response to environmental stressors. This study provides insights into radiation, BMT, and gut microbiota, highlighting the need for further research to understand their complex interactions.

Data availability statement

The sequencing data presented in the study are deposited in the European Nucleotide Archive (project accession number: PRJEB75490, https://www.ebi.ac.uk/ena/submit/webin/report/runs/ERP160066). Sample metadata and ENA accessions are listed in Supplementary Table S1.

Ethics statement

The animal study was approved by The Babraham Institute Animal Welfare and Ethical Review Body. The study was conducted in accordance with the local legislation and institutional requirements.

Author contributions

JK: Data curation, Formal analysis, Investigation, Methodology, Writing – original draft, Writing – review & editing, Software, Visualization. JD: Investigation, Writing – review & editing. KS: Investigation, Writing – review & editing. DČ: Investigation, Writing – review & editing. LS: Investigation, Writing – review & editing. BB: Investigation, Writing – review & editing. AL: Supervision, Writing – review & editing. AM: Supervision, Writing – review & editing, Conceptualization, Data curation, Formal analysis, Funding acquisition, Investigation, Methodology, Project administration, Resources, Writing – original draft.

Funding

Conflict of interest

The authors declare that the research was conducted in the absence of any commercial or financial relationships that could be construed as a potential conflict of interest.

Publisher's note

Supplementary material

The Supplementary material for this article can be found online at: https://www.frontiersin.org/articles/10.3389/fmicb.2024.1324403/full#supplementary-material

SUPPLEMENTARY FIGURE S1
[Caecum_ileum_overview.pdf]: Differences in gut microbiota between caecum and ileum. Consistently for all experimental groups, the microbiota of the ileum showed a lower alpha diversity and a different composition than the microbiota of the caecum. This is shown by **(A)** violin plots visualizing the differences in ASV richness, **(B)** Principal Coordinate analysis for Bray-Curtis dissimilarities, where caecum and ileum samples form non-overlapping clusters and where identity with the experimental group is indicated by Harwestman plots, and **(C)** bar charts showing the proportions of the 20 most abundant bacterial genera in each sample.

SUPPLEMENTARY FIGURE S2
[BETA_all.bc.pdf]: Differences in microbiota composition between non-irradiated controls and depleted or non-depleted mice exposed to radiation. Shifts in the composition of the microbiota of **(A)** cecum and **(B)** ileum between treatment groups were analyzed by PCoA ordination of Bray-Curtis dissimilarities. Treatment levels are indicated by different colors. Harwestman diagrams connect samples from the same treatment replicate. Interindividual variation for each treatment group is represented for **(C)** caecum and **(D)** ileum samples by violin plots showing the distribution of Bray-Curtis-based distances to the group-specific centroids. The horizontal lines within the violin plots correspond to the median values. Horizontal lines above the violin plots indicate significant differences between the experimental groups.

SUPPLEMENTARY FIGURE S3
[Bray_dose.pdf]: PCoA ordination of Bray-Crutis dissimilarities depicts variation in appendix microbiota composition between depleted and non-depleted mice exposed to either high or low doses of radiation.

SUPPLEMENTARY FIGURE S4
[BETA_all.bc_METAG.pdf]: Variation in predicted metagenome content of **(A)** caecum and **(B)** ileum between treatment groups, assessed based on PCoA for Bray-Curtis dissimilarities.

SUPPLEMENTARY FIGURE S5
[Bray_dose_METAG.pdf]: PCoA ordination of Bray-Curtis dissimilarities showing the differences in the composition of predicted cecal metagenomes between depleted and non-depleted mice exposed to either high or low doses of radiation.

SUPPLEMENTARY FIGURE S6
[DFA_all_METAG.pdf] Effect of radiation on predicted relative frequencies of phenotypic traits in caecum (CW) and ileum (IW) in controls and depleted or non-depleted irradiated mice. The differences between the three treatment groups were not statistically significant.

SUPPLEMENTARY FIGURE S7
[DFA_depl_nondepl_METAG] Effect of radiation dose and depletion treatment on the predicted relative abundances of metabolic pathways. Boxplots showing the variation of metabolic pathways whose relative abundance in the cecum of **(A)** the depleted group and **(B)** the non-depleted group differed between individuals exposed to low and high radiation dose.

References

Aguilera, M., Cerdà-Cuéllar, M., and Martínez, V. (2015). Antibiotic-induced dysbiosis alters host-bacterial interactions and leads to colonic sensory and motor changes in mice. *Gut Microbes* 6:10–23. doi: 10.4161/19490976.2014.990790

Benjamini, Y., and Hochberg, Y. (1995). Controlling the false discovery rate: a practical and powerful approach to multiple testing. *J. R. Stat. Soc. Series B (Methodological)* 57, 289–300. doi: 10.1111/j.2517-6161.1995.tb02031.x

Biagi, E., Zama, D., Nastasi, C., Consolandi, C., Fiori, J., Rampelli, S., et al. (2015). Gut microbiota trajectory in pediatric patients undergoing hematopoietic SCT. *Bone Marrow Transplant.* 50, 992–998. doi: 10.1038/bmt.2015.16

Biagi, E., Zama, D., Rampelli, S., Turroni, S., Brigidi, P., Consolandi, C., et al. (2019). Early gut microbiota signature of aGvHD in children given allogeneic hematopoietic cell transplantation for hematological disorders. *BMC Med. Genet.* 12:49. doi: 10.1186/s12920-019-0494-7

Callahan, B. J., McMurdie, P. J., Rosen, M. J., Han, A. W., Johnson, A. J. A., and Holmes, S. P. (2016). DADA2: high-resolution sample inference from Illumina amplicon data. *Nat. Methods* 13, 581–583. doi: 10.1038/nmeth.3869

Cani, P. D., Depommier, C., Derrien, M., Everard, A., and de Vos, W. M. (2022). *Akkermansia muciniphila*: paradigm for next-generation beneficial microorganisms. *Nat. Rev. Gastroenterol. Hepatol.* 19, 625–637. doi: 10.1038/s41575-022-00631-9

Čížková, D., Ďureje, Ľ., Piálek, J., and Kreisinger, J. (2021). Experimental validation of small mammal gut microbiota sampling from faeces and from the caecum after death. *Heredity* 127, 141–150. doi: 10.1038/s41437-021-00445-6

Cui, M., Xiao, H., Li, Y., Zhou, L., Zhao, S., Luo, D., et al. (2017). Faecal microbiota transplantation protects against radiation-induced toxicity. *EMBO Mol. Med.* 9, 448–461. doi: 10.15252/emmm.201606932

Daniele, N., Scerpa, M. C., Caniglia, M., Ciammetti, C., Rossi, C., Bernardo, M. E., et al. (2012). Overview of T-cell depletion in haploidentical stem cell transplantation. *Blood Transfus.* 10, 264–272. doi: 10.2450/2012.0106-11

Doki, N., Suyama, M., Sasajima, S., Ota, J., Igarashi, A., Mimura, I., et al. (2017). Clinical impact of pre-transplant gut microbial diversity on outcomes of allogeneic hematopoietic stem cell transplantation. *Ann. Hematol.* 96, 1517–1523. doi: 10.1007/s00277-017-3069-8

Douglas, G. M., Maffei, V. J., Zaneveld, J. R., Yurgel, S. N., Brown, J. R., Taylor, C. M., et al. (2020). PICRUSt2 for prediction of metagenome functions. *Nat. Biotechnol.* 38, 685–688. doi: 10.1038/s41587-020-0548-6

Edgar, R. C., Haas, B. J., Clemente, J. C., Quince, C., and Knight, R. (2011). UCHIME improves sensitivity and speed of chimera detection. *Bioinformatics* 27, 2194–2200. doi: 10.1093/bioinformatics/btr381

Eriguchi, Y., Takashima, S., Oka, H., Shimoji, S., Nakamura, K., Uryu, H., et al. (2012). Graft-versus-host disease disrupts intestinal microbial ecology by inhibiting Paneth cell production of α-defensins. *Blood* 120, 223–231. doi: 10.1182/blood-2011-12-401166

Fredricks, D. N. (2019). The gut microbiota and graft-versus-host disease. *J. Clin. Invest.* 129, 1808–1817. doi: 10.1172/JCI125797

Guo, H., Chou, W.-C., Lai, Y., Liang, K., Tam, J. W., Brickey, W. J., et al. (2020). Multi-omics analyses of radiation survivors identify radioprotective microbes and metabolites. *Science* 370:eaay9097. doi: 10.1126/science.aay9097

Ho, V. T., and Soiffer, R. J. (2001). The history and future of T-cell depletion as graft-versus-host disease prophylaxis for allogeneic hematopoietic stem cell transplantation. *Blood* 98, 3192–3204. doi: 10.1182/blood.V98.12.3192

Holler, E., Butzhammer, P., Schmid, K., Hundsrucker, C., Koestler, J., Peter, K., et al. (2014). Metagenomic analysis of the stool microbiome in patients receiving allogeneic stem cell transplantation: loss of diversity is associated with use of systemic antibiotics and more pronounced in gastrointestinal graft-versus-host disease. *Biol. Blood Marrow Transplant.* 20, 640–645. doi: 10.1016/j.bbmt.2014.01.030

Ingham, A. C., Kielsen, K., Cilieborg, M. S., Lund, O., Holmes, S., Aarestrup, F. M., et al. (2019). Specific gut microbiome members are associated with distinct immune markers in pediatric allogeneic hematopoietic stem cell transplantation. *Microbiome* 7:131. doi: 10.1186/s40168-019-0745-z

Ingham, A. C., Kielsen, K., Mordhorst, H., Ifversen, M., Aarestrup, F. M., Müller, K. G., et al. (2021). Microbiota long-term dynamics and prediction of acute graft-versus-host disease in pediatric allogeneic stem cell transplantation. *Microbiome* 9:148. doi: 10.1186/s40168-021-01100-2

Jenq, R. R., Ubeda, C., Taur, Y., Menezes, C. C., Khanin, R., Dudakov, J. A., et al. (2012). Regulation of intestinal inflammation by microbiota following allogeneic bone marrow transplantation. *J. Exp. Med.* 209, 903–911. doi: 10.1084/jem.20112408

Jiang, H., Lei, R., Ding, S. W., and Zhu, S. (2014). Skewer: a fast and accurate adapter trimmer for next-generation sequencing paired-end reads. *BMC Bioinformatics* 15:182. doi: 10.1186/1471-2105-15-182

Kastl, A. J., Terry, N. A., Wu, G. D., and Albenberg, L. G. (2020). The structure and function of the human small intestinal microbiota: current understanding and future directions. *Cell. Mol. Gastroenterol. Hepatol.* 9, 33–45. doi: 10.1016/j.jcmgh.2019.07.006

Katiraei, S., van Diepen, J. A., Tavares, L. P., Hoving, L. R., Pronk, A., Verschueren, I., et al. (2022). Bone marrow transplantation induces changes in the gut microbiota that chronically increase the cytokine response pattern of splenocytes. *Sci. Rep.* 12:6883. doi: 10.1038/s41598-022-10637-7

Kaysen, A., Heintz-Buschart, A., Muller, E. E. L., Narayanasamy, S., Wampach, L., Laczny, C. C., et al. (2017). Integrated meta-omic analyses of the gastrointestinal tract microbiome in patients undergoing allogeneic hematopoietic stem cell transplantation. *Transl. Res.* 186, 79–94.e1. doi: 10.1016/j.trsl.2017.06.008

Klindworth, A., Pruesse, E., Schweer, T., Peplies, J., Quast, C., Horn, M., et al. (2013). Evaluation of general 16S ribosomal RNA gene PCR primers for classical and next-generation sequencing-based diversity studies. *Nucleic Acids Res.* 41:e1. doi: 10.1093/nar/gks808

Kouidhi, S., Souai, N., Zidi, O., Mosbah, A., Lakhal, A., Ben Othmane, T., et al. (2021). High throughput analysis reveals changes in gut microbiota and specific fecal Metabolomic signature in hematopoietic stem cell transplant patients. *Microorganisms* 9:1845. doi: 10.3390/microorganisms9091845

Liu, J., Liu, C., and Yue, J. (2021). Radiotherapy and the gut microbiome: facts and fiction. *Radiat. Oncol.* 16:9. doi: 10.1186/s13014-020-01735-9

Lu, W., Qian, L., Fang, Z., Wang, H., Zhu, J., Lee, Y. K., et al. (2022). Probiotic strains alleviated OVA-induced food allergy in mice by regulating the gut microbiota and improving the level of indoleacrylic acid in fecal samples. *Food Funct.* 13, 3704–3719. doi: 10.1039/d1fo03520g

Mähler Convenor, M., Berard, M., Feinstein, R., Gallagher, A., Illgen-Wilcke, B., Pritchett-Corning, K., et al. (2014). FELASA recommendations for the health monitoring of mouse, rat, hamster, guinea pig and rabbit colonies in breeding and experimental units. *Lab. Anim.* 48, 178–192. doi: 10.1177/0023677213516312

Mancini, N., Greco, R., Pasciuta, R., Barbanti, M. C., Pini, G., Morrow, O. B., et al. (2017). Enteric microbiome markers as early predictors of clinical outcome in allogeneic hematopoietic stem cell transplant: results of a prospective study in adult patients. *Open Forum Infect. Dis.* 4:ofx215. doi: 10.1093/ofid/ofx215

McArtor, D. B., Lubke, G. H., and Bergeman, C. S. (2017). Extending multivariate distance matrix regression with an effect size measure and the asymptotic null distribution of the test statistic. *Psychometrika* 82, 1052–1077. doi: 10.1007/s11336-016-9527-8

Miltiadous, O., Waters, N. R., Andrlová, H., Dai, A., Nguyen, C. L., Burgos da Silva, M., et al. (2022). Early intestinal microbial features are associated with CD4 T-cell recovery after allogeneic hematopoietic transplant. *Blood* 139, 2758–2769. doi: 10.1182/blood.2021014255

Morjaria, S., Schluter, J., Taylor, B. P., Littmann, E. R., Carter, R. A., Fontana, E., et al. (2019). Antibiotic-induced shifts in fecal microbiota density and composition during hematopoietic stem cell transplantation. *Infect. Immun.* 87, e00206–e00219. doi: 10.1128/IAI.00206-19

Moudra, A., Niederlova, V., Novotny, J., Schmiedova, L., Kubovciak, J., Matejkova, T., et al. (2021). Phenotypic and clonal stability of antigen-inexperienced memory-like T cells across the genetic background, hygienic status, and aging. *J. Immunol.* 206, 2109–2121. doi: 10.4049/jimmunol.2001028

Parada Venegas, D., de la Fuente, M. K., Landskron, G., González, M. J., Quera, R., Dijkstra, G., et al. (2019). Short chain fatty acids (SCFAs)-mediated gut epithelial and immune regulation and its relevance for inflammatory bowel diseases. *Front. Immunol.* 10:277:277. doi: 10.3389/fimmu.2019.00277

Payen, M., Nicolis, I., Robin, M., Michonneau, D., Delannoye, J., Mayeur, C., et al. (2020). Functional and phylogenetic alterations in gut microbiome are linked to graft-versus-host disease severity. *Blood Adv.* 4, 1824–1832. doi: 10.1182/bloodadvances.2020001531

Peled, J. U., Gomes, A. L. C., Devlin, S. M., Littmann, E. R., Taur, Y., Sung, A. D., et al. (2020). Microbiota as predictor of mortality in allogeneic hematopoietic-cell transplantation. *N. Engl. J. Med.* 382, 822–834. doi: 10.1056/NEJMoa1900623

Quast, C., Pruesse, E., Yilmaz, P., Gerken, J., Schweer, T., Yarza, P., et al. (2013). The SILVA ribosomal RNA gene database project: improved data processing and web-based tools. *Nucleic Acids Res.* 41, D590–D596. doi: 10.1093/nar/gks1219

Sen, T., and Thummer, R. P. (2022). The impact of human microbiotas in hematopoietic stem cell and organ transplantation. *Front. Immunol.* 13:932228. doi: 10.3389/fimmu.2022.932228 (Accessed: 9 June 2023)

Song, Q., Cheng, S. W., Li, D., Cheng, H., Lai, Y. S., Han, Q., et al. (2022). Gut microbiota mediated hypoglycemic effect of *Astragalus membranaceus* polysaccharides in db/db mice. *Front. Pharmacol.* 13:1043527. doi: 10.3389/fphar.2022.1043527

Staffas, A., Burgos da Silva, M., and van den Brink, M. R. M. (2017). The intestinal microbiota in allogeneic hematopoietic cell transplant and graft-versus-host disease. *Blood* 129, 927–933. doi: 10.1182/blood-2016-09-691394

Styczyński, J., Tridello, G., Koster, L., Iacobelli, S., van Biezen, A., van der Werf, S., et al. (2020). Death after hematopoietic stem cell transplantation: changes over calendar year time, infections and associated factors. *Bone Marrow Transplant.* 55, 126–136. doi: 10.1038/s41409-019-0624-z

Taur, Y., Xavier, J. B., Lipuma, L., Ubeda, C., Goldberg, J., Gobourne, A., et al. (2012). Intestinal domination and the risk of bacteremia in patients undergoing allogeneic hematopoietic stem cell transplantation. *Clin. Infect. Dis.* 55, 905–914. doi: 10.1093/cid/cis580

Wang, Q., Garrity, G. M., Tiedje, J. M., and Cole, J. R. (2007). Naive Bayesian classifier for rapid assignment of rRNA sequences into the new bacterial taxonomy. *Appl. Environ. Microbiol.* 73, 5261–5267. doi: 10.1128/AEM.00062-07

Ward, T., Larson, J., Meulemans, J., Hillmann, B., Lynch, J., Sidiropoulos, D., et al. (2017). BugBase predicts organism-level microbiome phenotypes. *bioRxiv* 2017:133462. doi: 10.1101/133462

Weber, D., Hiergeist, A., Weber, M., Dettmer, K., Wolff, D., Hahn, J., et al. (2019). Detrimental effect of broad-spectrum antibiotics on intestinal microbiome diversity in patients after allogeneic stem cell transplantation: lack of commensal sparing antibiotics. *Clin. Infect. Dis.* 68, 1303–1310. doi: 10.1093/cid/ciy711

Ye, Y., and Doak, T. G. (2009). A parsimony approach to biological pathway reconstruction/inference for genomes and metagenomes. *PLoS Comput. Biol.* 5:e1000465. doi: 10.1371/journal.pcbi.1000465

Zagato, E., Pozzi, C., Bertocchi, A., Schioppa, T., Saccheri, F., Guglietta, S., et al. (2020). Endogenous murine microbiota member Faecalibaculum rodentium and its human homologue protect from intestinal tumour growth. *Nat. Microbiol.* 5, 511–524. doi: 10.1038/s41564-019-0649-5

Zama, D., Bossù, G., Leardini, D., Muratore, E., Biagi, E., Prete, A., et al. (2020). Insights into the role of intestinal microbiota in hematopoietic stem-cell transplantation. *Ther. Adv. Hematol.* 11:96961. doi: 10.1177/2040620719896961

Zaneveld, J. R., McMinds, R., and Vega Thurber, R. (2017). Stress and stability: applying the Anna Karenina principle to animal microbiomes. *Nat. Microbiol.* 2:17121. doi: 10.1038/nmicrobiol.2017.121

Zoetendal, E. G., Raes, J., van den Bogert, B., Arumugam, M., Booijink, C. C. G. M., Troost, F. J., et al. (2012). The human small intestinal microbiota is driven by rapid uptake and conversion of simple carbohydrates. *ISME J.* 6, 1415–1426. doi: 10.1038/ismej.2011.212